The Journal of Chemical Physics

Long-lived quantum coherent dynamics of a Λ-system driven by a thermal environment

Cite as: J. Chem. Phys. **157**, 124302 (2022); https://doi.org/10.1063/5.0102808
Submitted: 13 June 2022 • Accepted: 24 August 2022 • Published Online: 23 September 2022

Suyesh Koyu and Timur V. Tscherbul

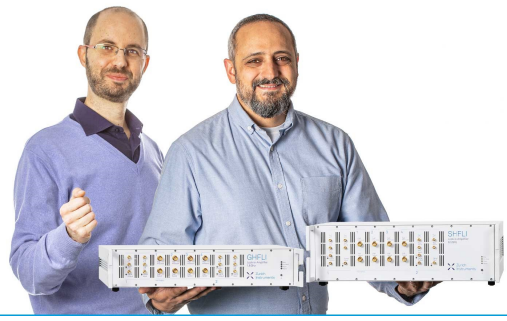

The Journal of Chemical Physics ARTICLE scitation.org/journal/jcp

Long-lived quantum coherent dynamics of a Λ-system driven by a thermal environment

Cite as: J. Chem. Phys. 157, 124302 (2022); doi: 10.1063/5.0102808
Submitted: 13 June 2022 • Accepted: 24 August 2022 •
Published Online: 23 September 2022

Suyesh Koyu and Timur V. Tscherbul[a)]

AFFILIATIONS

Department of Physics, University of Nevada, Reno, Nevada 89557, USA

[a)]Author to whom correspondence should be addressed: ttscherbul@unr.edu

ABSTRACT

We present a theoretical study of quantum coherent dynamics of a three-level Λ-system driven by a thermal environment (such as blackbody radiation), which serves as an essential building block of photosynthetic light-harvesting models and quantum heat engines. By solving nonsecular Bloch–Redfield master equations, we obtain analytical results for the ground-state population and coherence dynamics and classify the dynamical regimes of the incoherently driven Λ-system as underdamped and overdamped depending on whether the ratio $\Delta/[rf(p)]$ is greater or less than one, where Δ is the ground-state energy splitting, r is the incoherent pumping rate, and $f(p)$ is a function of the transition dipole alignment parameter p. In the underdamped regime, we observe long-lived coherent dynamics that lasts for $\tau_c \simeq 1/r$, even though the initial state of the Λ-system contains no coherences in the energy basis. In the overdamped regime for $p = 1$, we observe the emergence of coherent quasi-steady states with the lifetime $\tau_c = 1.34(r/\Delta^2)$, which have a low von Neumann entropy compared to conventional thermal states. We propose an experimental scenario for observing noise-induced coherent dynamics in metastable He^* atoms driven by x-polarized incoherent light. Our results suggest that thermal excitations can generate experimentally observable long-lived quantum coherent dynamics in the ground-state subspace of atomic and molecular Λ-systems in the absence of coherent driving.

I. INTRODUCTION

The quantum dynamics of multilevel atoms and molecules interacting with noisy electromagnetic fields [most notably, blackbody radiation (BBR)] plays a central role in photosynthetic energy transfer in biological systems,[1–5] quantum thermodynamics,[6–8] and precision measurement.[9–12] In particular, the essential first steps in photosynthetic energy transfer[1,13–17] and in vision[18–22] involve photoexcitation of biological chromophore molecules by incoherent solar light, which can be approximated as a BBR source.[13,14] The role of quantum coherence in these primary biological processes remains incompletely understood and continues to attract significant interest.[1–3] In addition, BBR shifts atomic and molecular energy levels and causes incoherent transitions between them, limiting the precision of highly accurate spectroscopic measurements.[9–12]

The standard theoretical treatment of quantum dynamics of multilevel atoms and molecules driven by the blackbody radiation is based on solving secular (Pauli) rate equations[23,24] for the time evolution of state populations. While adequate in many cases of practical interest, the rate equations rely on the secular approximation, which neglects the coherences between the atomic and/or molecular energy levels.[23,24] The secular approximation cannot be justified in the presence of nearly degenerate energy levels (also known as Liouvillian degeneracies[25]), in which case the more sophisticated Bloch–Redfield (BR) master equations, which account for the population-to-coherence coupling terms, should be used.[4,26–35] The population-to-coherence couplings lead to interesting and underexplored physical effects, such as the generation of noise-induced quantum coherences by thermal driving alone (i.e., in the absence of coherent driving) starting from a coherence-free initial state.[4,7,8,27–29,36–40] These noise-induced Fano coherences arise due to the interference of different incoherent transition pathways[3,4,27,30] caused by the cross-coupling terms in the light–matter interaction Hamiltonian of the form $\boldsymbol{\mu}_{ik} \cdot \boldsymbol{\mu}_{jk}$,[41] where $\boldsymbol{\mu}_{ij} = \langle i|\boldsymbol{\mu}|j\rangle$ are the transition dipole matrix elements in the system eigenstate basis. Physically, these cross couplings arise from the transitions $k \leftrightarrow i$ and $k \leftrightarrow j$ being driven by the same mode of the incoherent radiation field.[3] Importantly, these couplings

do not average to zero under isotropic incoherent excitation if the corresponding transition dipole moments are non-orthogonal ($\boldsymbol{\mu}_{ik} \cdot \boldsymbol{\mu}_{jk} \neq 0$).[4,42]

Early theoretical studies of Fano coherences focused on coherent population trapping and resonance fluorescence of trapped ions.[36,37] The authors of Ref. 36 considered a four-level system driven by polarized incoherent radiation in addition to a coherent pump field and proposed it for lasing without inversion. More recent theoretical work investigated the role of Fano coherences in suppressing spontaneous emission from three-level atoms,[43] in enhancing the efficiency of quantum heat engines,[7,8] in biological processes induced by solar light,[1,15,16,44–46] and in negative entropy production.[47] We have explored the dynamical evolution of Fano coherences in a model three-level V-system excited by isotropic[4,27,29] and polarized[28,40] incoherent light. In the latter case, we studied the properties of coherent quasi-steady states,[48] which form in the long-time limit and differ substantially from the conventional thermal states predicted by the secular rate equations. Recently, closely related vacuum-induced Fano coherences have been detected experimentally in a cold ensemble of Rb atoms.[49]

A three-level Λ-system consisting of two nearly degenerate ground levels radiatively coupled to a single excited level [see Fig. 1(a)] is a paradigmatic quantum multilevel system, which serves as a fundamental building block of photosynthetic light-harvesting complexes,[1,15–17] quantum heat engines,[7,8] and quantum optical systems.[50] However, despite its profound significance, the thermally driven Λ-system has only been explored in the regime of degenerate ground levels ($\Delta = 0$),[39] which is a theoretical idealization due to the presence of degeneracy-lifting Stark and Lamb shifts.[41,51] This leaves open the question of whether thermal environments can induce and sustain coherent ground-state dynamics in realistic atomic and/or molecular Λ-systems.

Here, we study the quantum dynamics of the Λ-system driven by a thermal environment, such as BBR. By solving nonsecular Bloch–Redfield quantum master equations, we obtain analytic results for the time evolution of noise-induced Fano coherences between the ground levels of the Λ-system and establish the existence of two distinct dynamical regimes, where the coherences exhibit either long-lived underdamped oscillations or quasi-steady states with a low entropy compared to the conventional thermal

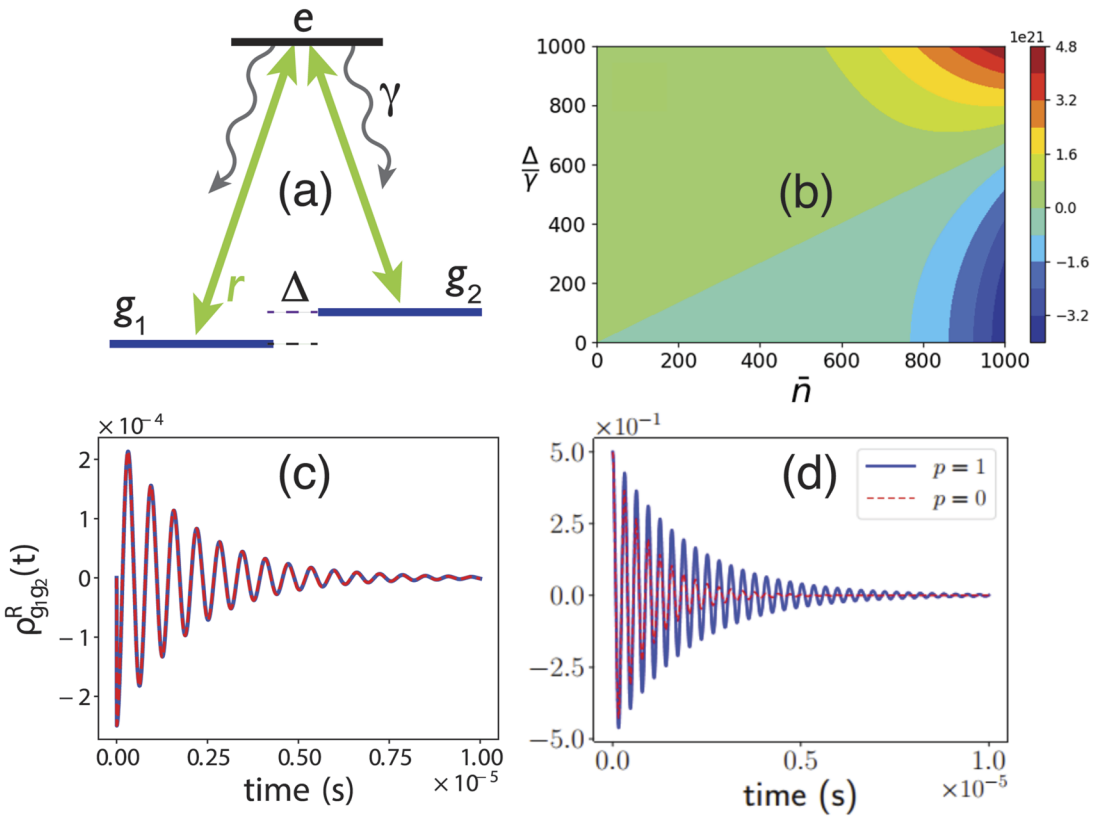

FIG. 1. (a) Schematic diagram of the Λ-system with two ground states $|g_1\rangle$ and $|g_2\rangle$ and a single excited state $|e\rangle$. (b) The discriminant D as a function of the average photon number $\bar{n}$ and the reduced splitting Δ/γ showing the different dynamical regimes of the incoherently driven Λ-system. Regions of positive D correspond to the underdamped regime; those of negative D correspond to the overdamped regime. (c) Coherence dynamics of the Λ-system initially in the fully mixed thermal state [$\rho_{g_ig_i}(0) = 1/2$ and $\rho_{g_1g_2}(0) = 0$] for $\Delta/\gamma = 10^{-2}$, $\gamma = 10^9\ \mathrm{s}^{-1}$, $\bar{n} = 10^{-3}$, and $p = 1$. Full lines represent numerically exact results, dashed lines represent analytical results. (d) Same as (c) for the initial coherent superposition [$\rho_{g_1g_2}(0) = 1/2$] with $p = 1$ (full line) and $p = 0$ (dashed line) for $\Delta/\gamma = 2 \times 10^{-2}$ and $\bar{n} = 10^{-3}$.

states. Our results show that it is possible to generate long-lived quantum coherent dynamics between the ground states of the Λ-system using solely BBR driving, and we suggest an experimental scenario for observing this dynamics (along with the resultant coherent steady states) in metastable He^* atoms in an external magnetic field.

The rest of this paper is structured as follows. In Sec. II A, we formulate the theory of incoherent excitation of the Λ-system using the Bloch–Redfied quantum master equations and present their analytical solutions. In Sec. II B, we discuss two primary regimes of population and coherence dynamics (underdamped and overdamped). In Sec. III, we suggest an experimental scenario for observing noise-induced Fano coherences in the steady state using metastable He^* atoms driven by polarized incoherent BBR. Section IV concludes by summarizing the main results of this work.

II. NOISE-INDUCED COHERENT DYNAMICS

A. Theory: Bloch–Redfield master equations and their analytical solution

The energy level structure of the Λ-system, shown in Fig. 1(a), consists of two nearly degenerate ground states $|g_1\rangle$ and $|g_2\rangle$ coupled to a single excited state $|e\rangle$ by the incoherent radiation field. As pointed out in the Introduction, the Λ level structure can be regarded as a minimal model of a multilevel quantum system interacting with incoherent BBR. (Another widely used minimal model is the three-level V-system considered elsewhere.[4,27]) The quantum dynamics of the Λ-system driven by isotropic incoherent radiation is described by Bloch–Redfield (BR) quantum master equations for the density matrix in the eigenstate basis,[30,39]

$$\begin{aligned}\dot\rho_{g_ig_i} &= -r_i\rho_{g_ig_i} + (r_i+\gamma_i)\rho_{ee} - p\sqrt{r_1r_2}\rho^R_{g_1g_2},\\ \dot\rho_{g_1g_2} &= -i\rho_{g_1g_2}\Delta - \frac{1}{2}(r_1+r_2)\rho_{g_1g_2}\\ &\quad + p(\sqrt{r_1r_2}+\sqrt{\gamma_1\gamma_2})\rho_{ee} - \frac{p}{2}\sqrt{r_1r_2}(\rho_{g_1g_1}+\rho_{g_2g_2}),\end{aligned} \tag{1}$$

where $\rho_{g_ig_i}$ are the ground-state populations, $\rho_{g_1g_2} = \rho^R_{g_1g_2} + i\rho^I_{g_1g_2}$ is the coherence between the ground states $|g_1\rangle$ and $|g_2\rangle$ [see Fig. 1(a)] with the real and imaginary parts $\rho^R_{g_1g_2}$ and $\rho^I_{g_1g_2}$, γ_i is the radiative decay rate of the excited state $|e\rangle$ into the ground state $|i\rangle$, $r_i = \bar n\gamma_i$ is the incoherent pumping rate, $\bar n$ is the average occupation number of the thermal field ($\bar n \simeq 10^{-9}$ for typical sunlight-harvesting conditions[4,52]), $p = (\boldsymbol{\mu}_{g_1e}\cdot\boldsymbol{\mu}_{g_2e})/\mu_{g_1e}\mu_{g_2e}$ is the transition dipole alignment factor, and $\boldsymbol{\mu}_{ij}$ is the transition dipole matrix element between the states i and j.

We consider a symmetric Λ-system ($r_1 = r_2 = r$) driven by a suddenly turned on incoherent light. This restriction drastically simplifies the solution of BR equations without losing the essential physics.[4,27] Equation (1) relies on the Born–Markov approximation, which is known to be very accurate for quantum optical systems.[53] Significantly, we do not assume the validity of the secular approximation, which cannot be justified for nearly degenerate energy levels.[4,26–35] This approximation is equivalent to setting $p = 0$ in Eq. (1), which eliminates the population-to-coherence coupling terms and, hence, Fano coherences (see below). Several authors have shown that nonsecular BR equations[4,30–35] and related Lindblad-form master equations[54] generally provide a more accurate description of open quantum system dynamics than secular rate equations.

To solve BR equations (1), we recast them in the matrix form $\dot{\mathbf{x}}(t) = \mathbf{A}\mathbf{x}(t) + \mathbf{d}$, where $\mathbf{x}(t) = (\rho_{g_1g_1}, \rho^R_{g_1g_2}, \rho^I_{g_1g_2})^T$ is the state vector in the Liouville representation, $\mathbf{A}$ is the matrix of coefficients on the right-hand side of Eq. (1), $\mathbf{d}$ is a constant driving vector, and $\mathbf{x}_0$ defines the initial conditions for the density matrix. The solutions of the matrix BR equation $\mathbf{x}(t) = e^{\mathbf{A}t}\mathbf{x}_0 + \int_0^\infty ds e^{\mathbf{A}(t-s)}\mathbf{d}$ may be expressed in terms of the eigenvalues of $\mathbf{A}$, which determine the decay timescales of the different eigenmodes of the system. The general features of the solutions can be understood without finding the eigenvalues by considering the discriminant of the characteristic equation (see the supplementary material),

$$D = B^3 + \left[C - \frac{3}{2}A(B+A^2)\right]^2, \tag{2}$$

where $A = \frac{1}{3}(5r+2\gamma)$, $B = \frac{1}{3}\left[\Delta^2 + r^2 + (2-p^2)r(3r+2\gamma)\right] - A^2$, and $C = \frac{1}{2}(3r+2\gamma)\left[\Delta^2 + (1-p^2)r^2\right] + A^3$. The three dynamical regimes can be distinguished depending on the sign of D using the analogy with the damped harmonic oscillator.[27] In the underdamped regime ($D > 0$), $\mathbf{A}$ has one negative real and two complex conjugate eigenvalues, giving rise to exponentially decaying and two oscillating eigenmodes. In the overdamped regime ($D < 0$), all of the eigenvalues are real and negative, and thus, the eigenmodes decay exponentially. In the critical regime ($D = 0$), all eigenvalues are real and negative, and at least two of them are equal.

As shown in the supplementary material, $D = \frac{\gamma^6}{2916}\sum_{k=0}^6 d_k(p, \frac{\Delta}{\gamma})\bar n^k$. Figure 1(b) illustrates the different dynamical regimes of the incoherently driven Λ-system obtained by solving the equation $D = 0$. We observe that the regions of positive D are separated from those of negative D by the critical line $\Delta/\gamma = f(p)\bar n$, where $f(p)$ is a universal function of p (see the supplementary material), which gives the slope of the line. Thus, *the overdamped regime is realized for* $\Delta/\gamma < f(p)\bar n$ *and the underdamped regime is realized for* $\Delta/\gamma > f(p)\bar n$.

In the limit $\bar n \to 0$, we obtain $D = \frac{\gamma^6}{27}(\frac{\Delta}{\gamma})^2[(\frac{\Delta}{\gamma})^2 + 4]^2 > 0$. Thus, as shown below, the Λ-system predominantly exhibits underdamped oscillatory dynamics under weak thermal driving, in marked contrast with the weakly driven V-system, where the underdamped regime is realized only for $\Delta/\gamma > 1$.[4,27,29] This is because the ground states of the Λ-system are not subject to spontaneous decay, unlike the excited states of the V-system. As a result, the two-photon coherence lifetime of the V-system scales as $1/\gamma$, whereas that of the Λ-system scales as $1/r$ [as follows from Eq. (1) for $p = 0$]. We note that while the overdamped regime does exist in the weakly driven Λ-system when $\Delta/r < p^2/2$ (see the supplementary material), it is a highly restrictive condition, so we limit our discussion below to underdamped dynamics.

The eigenvalues λ_j of $\mathbf{A}$ give the decay rates of the corresponding eigenmodes (see the supplementary material),

$$\lambda_j = -A + \alpha_j\frac{B}{\mathcal{T}} - \beta_j\mathcal{T}, \tag{3}$$

where $\mathcal{T} = \sqrt[3]{E+\sqrt{D}}$, $E = [C - \frac{3}{2}A(B+A^2)]$, $\omega = \frac{-1+i\sqrt{3}}{2}$, the quantities A, B, and C are defined below Eq. (2) and α_j and β_j are the cube roots of unity $[(\alpha_1,\beta_1) = (1,1), (\alpha_2,\beta_2) = (\omega^2,\omega)$, and $(\alpha_3,\beta_3) = (\omega,\omega^2)]$. We next consider the various limits of coherence dynamics defined by the sign of D.

In the *weakly driven regime* $(r/\gamma \ll 1)$, the general expressions (3) can be simplified to give $\lambda_1 = -(3r+2\gamma) = -2\gamma$ and $\lambda_{2,3} = -rQ(\frac{\Delta}{\gamma}) \pm i\Delta$, where $Q(x) \in [1/2, 1]$ is a smooth function, which increases monotonically with $x = \Delta/\gamma$. The general analytical solutions of the BR equations in the underdamped regime may be written as (see the supplementary material for a derivation)

$$\rho^R_{g_1g_2}(t) = \left[\rho^R_{g_1g_2}(0)\cos\Delta t + \rho^I_{g_1g_2}(0)\sin\Delta t\right]e^{-rQ\left(\frac{\Delta}{\gamma}\right)t} + \frac{pr}{2[4\gamma^2+\Delta^2]}\left[2\gamma e^{-2\gamma t} - (2\gamma\cos\Delta t + \Delta\sin\Delta t)e^{-rQ\left(\frac{\Delta}{\gamma}\right)t}\right],$$

$$\rho^I_{g_1g_2}(t) = \left[-\rho^R_{g_1g_2}(0)\sin\Delta t + \rho^I_{g_1g_2}(0)\cos\Delta t\right]e^{-rQ\left(\frac{\Delta}{\gamma}\right)t} + \frac{pr}{2[4\gamma^2+\Delta^2]}\left[\Delta e^{-2\gamma t} + (2\gamma\sin\Delta t - \Delta\cos\Delta t)e^{-rQ\left(\frac{\Delta}{\gamma}\right)t}\right]. \quad (4)$$

Here, $\rho_{ij}(0)$ specify the initial conditions for the density matrix of the Λ-system at $t = 0$, which we assume to be in an equal coherent superposition $[\rho_{g_1g_1}(0) = \rho_{g_2g_2}(0) = 1/2]$.

In the important particular case of a fully mixed, coherence-free initial state, we have $\rho_{g_1g_2}(0) = 0$ and $\rho_{g_ig_i}(0) = 1/2$, and Eq. (4) reduces to

$$\rho^R_{g_1g_2}(t) = \frac{pr}{2[4\gamma^2+\Delta^2]}\left[2\gamma e^{-2\gamma t} - (2\gamma\cos\Delta t + \Delta\sin\Delta t)e^{-rQ\left(\frac{\Delta}{\gamma}\right)t}\right],$$

$$\rho^I_{g_1g_2}(t) = \frac{pr}{2[4\gamma^2+\Delta^2]}\left[\Delta e^{-2\gamma t} + (2\gamma\sin\Delta t - \Delta\cos\Delta t)e^{-rQ\left(\frac{\Delta}{\gamma}\right)}\right]. \quad (5)$$

The concomitant population dynamics are given by

$$\rho_{g_1g_1}(t) = \frac{1}{(3r+2\gamma)}\left[r+\gamma+\frac{r}{2}e^{-2\gamma t}\right]. \quad (6)$$

B. Noise-induced coherent dynamics of the Λ-system

Figure 1(c) shows the ground-state population and coherence dynamics of the incoherently driven Λ-system initially in the incoherent mixture of the ground states $[\rho_{g_ig_i}(0) = 1/2]$ for $p = 1$ obtained by the numerical solution of BR equations. We observe that incoherent driving produces quantum beats due to Fano coherences *in the absence of initial coherence in the system*. The coherent oscillations decay on the timescale $\left[rQ(\frac{\Delta}{\gamma})\right]^{-1}$ in agreement with the analytical result (5). As the energy gap between the ground levels narrows down, the function $Q(\frac{\Delta}{\gamma})$ decreases from 1 to 1/2 (see the supplementary material), and the coherence lifetime increases by a factor of two. This is because the incoherent excitations $|g\rangle \leftrightarrow |e_i\rangle$ interfere more effectively at small Δ/γ,[40] as signaled by the non-negligible population-to-coherence coupling term $-p\sqrt{r_1r_2}\rho^R_{g_1g_2}$ in Eq. (1) in the limit $\Delta/\gamma \ll 1$. We note that if incoherent driving is turned on gradually (rather than suddenly, as assumed here), the quantum beats will become suppressed until they eventually disappear in the limit of adiabatically turned on incoherent driving.[55,56] However, steady-state Fano coherences generated by polarized incoherent excitation (see Sec. III) do survive the adiabatic turn-on.[40]

If the Λ-system is initialized in a coherent superposition of its ground states $[\rho_{g_1g_2}(0) = 1/2]$, the dynamics under incoherent driving is given by using Eq. (4) and contains additional terms proportional to $\rho_{g_1g_2}(0)$, which arise from the coherent initial condition (see the supplementary material). From Fig. 1(d), we observe that, in the absence of Fano interference $(p = 0)$, the initially excited coherent superposition decays on the timescale $1/r$ as expected due to incoherent transitions to the excited state $|g_i\rangle \to |e\rangle$ followed by spontaneous decay to the vacuum modes of the electromagnetic field [indeed, the analytical solution of the BR equations (1) for $p = 0$ is $\rho_{g_1g_2}(t) = \rho_{g_1g_2}(0)e^{-(i\Delta+r)t}$]. Thus, Fano interference generated by incoherent driving "extends" the lifetime of the initial coherent superposition due to the noise-induced contribution (5).

We now turn to the overdamped dynamics of the strongly driven Λ-system defined by the condition $\Delta/r < f(n)$. Expanding the eigenvalues of $\mathbf{A}$ in $1/\bar{n} \ll 1$, we find that λ_i do not depend on Δ/γ for $p < p_c$, where $p_c \simeq 1$ (see the supplementary material).[29] Remarkably, when the transition dipoles are nearly perfectly aligned $(p > p_c)$, the scaling changes dramatically to $\lambda_2 = -0.75\frac{\gamma}{\bar{n}}(\Delta/\gamma)^2$, giving rise to a coherent quasi-steady state with the lifetime $\tau_c = 1.34r/\Delta^2$ that increases without limit as $\Delta \to 0$. This point is illustrated in Figs. 2(a) and 2(b), where we plot the population and coherence dynamics of the Λ-system strongly driven by incoherent light. We observe that the coherences rise quickly from zero to an intermediate "plateau" value, where they remain for $t = \tau_c$ before eventually decaying back to zero. Our analytical results for coherence dynamics are in excellent agreement with numerical calculations, as shown in Figs. 2(a) and 2(b). They reduce to prior $\Delta = 0$ results[39] in the limit $\Delta \to 0$, where the quasi-steady states shown in Figs. 2(a) and 2(b) become true steady states.

To understand the physical origin of long-lived Fano coherences in the Λ-system, we use the effective decoherence rate model.[29] As shown in Fig. 2(c), the decay of the ground-state population $\rho_{g_ig_i}$ is accompanied by a steady growth of the population inversion $\rho_{ee} - \rho_{g_1g_1}$, which drives coherence generation. We observe that in the quasi-steady state, the time evolution of the population difference is identical to that of $\rho^R_{g_1g_2}$ and that $\rho^I_{g_1g_2}$ is time-independent. Neglecting the terms proportional to γ in Eq. (1), which is a good approximation in the strong pumping limit, and setting the left-land side of the resulting expression to zero, we obtain $\rho^I_{g_1g_2} = -(\Delta/r)\rho^R_{g_1g_2}$ (see the supplementary material). This leads to a simplified equation of motion for $\rho^R_{g_1g_2}$ valid at $t > 1/r$, $\dot{\rho}^R_{g_1g_2} = -r\left(1 - p + \Delta^2/r^2\right)\rho^R_{g_1g_2}$, which implies an exponential decay of the ground-state Fano coherence. The coherence lifetime

$$1/\tau_d^{\text{eff}} = r(1 - p + \Delta^2/r^2) \quad (7)$$

is consistent with the analytical result derived above. There are two distinct contributions to the overall decoherence rate in Eq. (7),

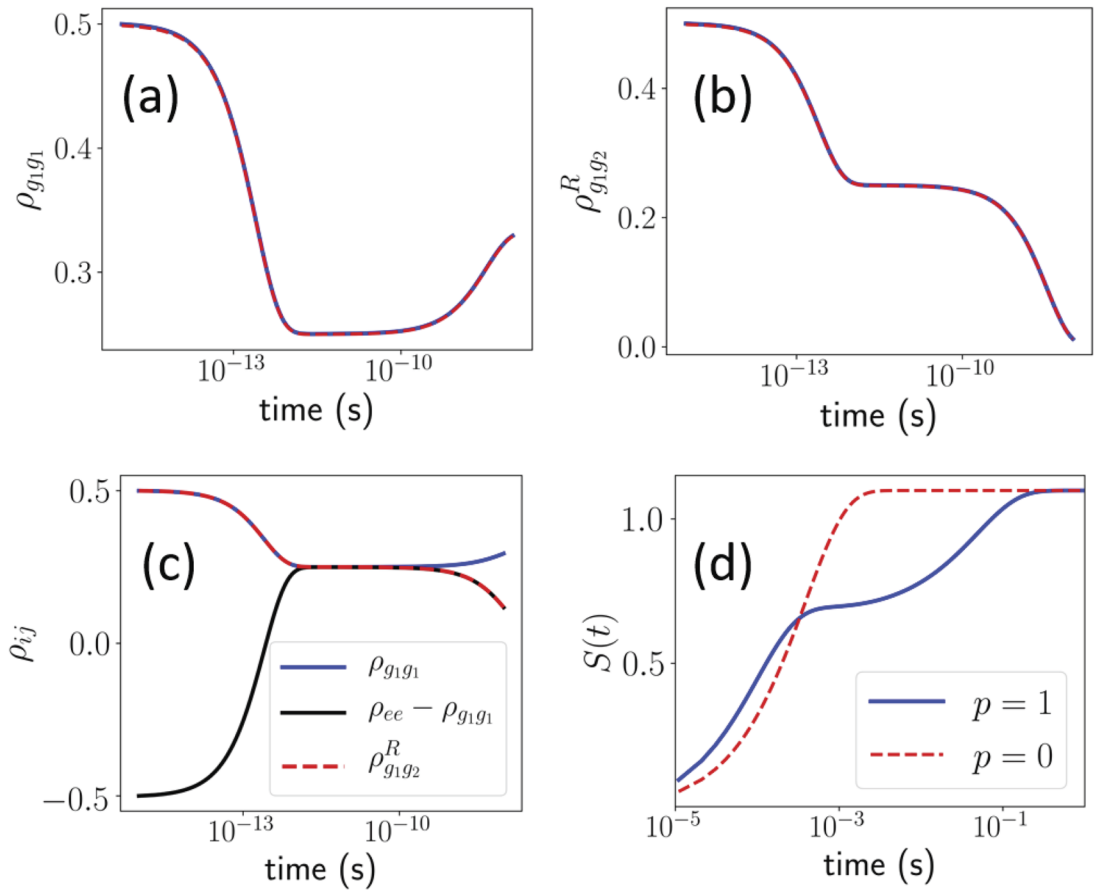

FIG. 2. Ground-state population (a), coherence (b), and population difference (c) dynamics of the Λ-system strongly driven by incoherent light ($\bar{n} = 10^3$, $\gamma = 10^9$ s^{-1}, $\Delta/\gamma = 10$, and $p = 1$). The Λ-system is initially in the fully mixed state $\rho(0) = \frac{1}{2}(|g_1\rangle\langle g_1| + |g_2\rangle\langle g_2|)$. (d) Time evolution of the von Neumann entropy with full Fano coherence [blue solid line] and without Fano coherence (red dashed line) for $\bar{n} = 10^3$ and $\Delta/\gamma = 10^2$. The ground states are initially in the coherent superposition $\rho(0) = \frac{1}{2}(|g_1\rangle\langle g_1| + |g_2\rangle\langle g_2| + |g_1\rangle\langle g_2| + |g_2\rangle\langle g_1|)$.

which are similar to those identified in our previous work on the V-system:[29] (i) the interplay between the coherence-generating Fano interference and incoherent stimulated emission [the term $r(1-p)$] and (ii) the coupling between the real and imaginary parts of the coherence due to the unitary evolution (the term Δ^2/r). The first mechanism does not contribute in the limit $p \to 1$, explaining the formation of the long-lived coherent quasi-steady state shown in Fig. 2, which decays via mechanism (ii) at a rate $\propto r/\Delta^2$.

Figure 2(d) shows the time evolution of the von Neumann entropy, $\mathcal{S}(t) = -\mathrm{Tr}(\rho \ln \rho)$, of the incoherently driven Λ-system calculated with $(p = 1)$ and without $(p = 0)$ Fano coherence. The analytic expression for the entropy in terms of the populations and coherences is given by (see the supplementary material)

$$\mathcal{S}(t) = -[(\rho_{g_1g_1} + |\rho_{g_1g_2}|)\ln(\rho_{g_1g_1} + |\rho_{g_1g_2}|) + (\rho_{g_1g_1} - |\rho_{g_1g_2}|)\ln(\rho_{g_1g_1} - |\rho_{g_1g_2}|) + \rho_{ee}\ln\rho_{ee}] \quad (8)$$

with $\rho_{ee} = 1 - \rho_{g_1g_1} - \rho_{g_2g_2}$. We observe that the entropy of the long-lived coherent quasi-steady state is two times smaller than that of the corresponding $p = 0$ thermal state due to the presence of substantial coherences in the energy basis. The low-entropy state persists for $\tau_c \propto (r/\Delta^2)$ before decaying to the high-entropy thermal state.

III. PROPOSAL FOR EXPERIMENTAL OBSERVATION OF FANO COHERENCES IN He* ATOMS

We finally turn to the question of the experimental observation of Fano coherences. We suggest metastable He(2^3S_1) atoms[57,58] as a readily realizable Λ-system, in which to observe noise-induced coherent dynamics. The Λ-system is formed by the $m = \pm 1$ Zeeman sublevels of the metastable ^3S state and the nondegenerate excited $^3P_0$ state, as shown in Fig. 3(a). The energy gap Δ between the Zeeman sublevels is continuously tunable with an external magnetic field, providing access to both the overdamped and underdamped regimes of coherence dynamics. The $^3S_{m=\pm1} \leftrightarrow {}^3P_0$

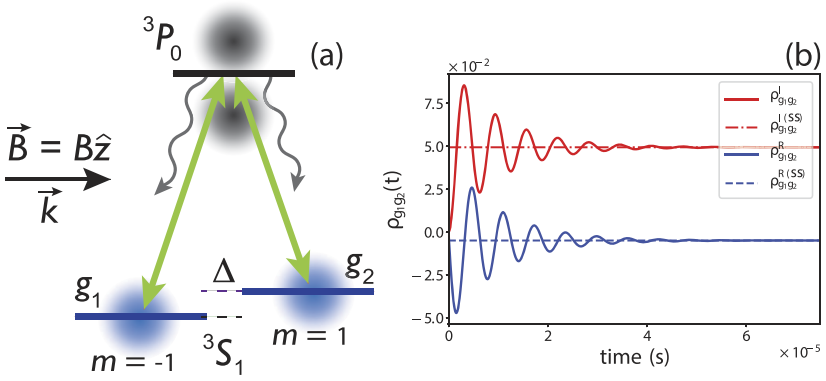

FIG. 3. (a) Schematic diagram of the Λ-system configuration to detect Fano coherences in He* atoms. The $^3S_{m=\pm1} \leftrightarrow {}^3P_0$ transitions are indicated by double-headed arrows. The magnetic field is parallel to the propagation vector of the *x*-polarized incoherent light, which defines the quantization axis. (b) Ground-state coherence dynamics of He* excited by *x*-polarized incoherent light with the parameters $\gamma = 10^8\ \mathrm{s}^{-1}$, $\bar{n} = 10^{-3}$, and $\Delta/\gamma = 10^{-2}$.

transitions are driven by a spectrally broadened laser field polarized in the *x*-direction. This excitation scheme allows us to (i) neglect radiative transitions involving the $m = 0$ ground-state Zeeman sublevel, thereby realizing an ideal three-level Λ-system (since He* has no hyperfine structure), and (ii) bypass the $p = 1$ condition needed to generate the Fano interference via isotropic incoherent excitation.[28,40] Because both of the Λ-system transitions couple to the same polarization mode of the incoherent radiation field, the BR equations (1) can be simplified by replacing $r + \gamma \to \gamma$ (see the supplementary material).[28,40]

Figure 3(b) shows the ground-state Fano coherence dynamics of a He* atom driven by *x*-polarized incoherent light starting from a coherence-free initial state $\rho_{g_ig_i}(0) = 1/2$. As in the case of isotropic incoherent excitation considered above, the coherences exhibit quantum beats with frequency Δ and lifetime $1/(Qr)$. The coherent evolution could be probed by applying a $\pi/2$ radiofrequency pulse (as part of the standard Ramsey sequence[58,59]) to convert the coherences to the populations of the $m = \pm1$ atomic states, which could be measured by, e.g., state-selective photoionization.[57,58]

Significantly, as shown in Fig. 3(b), the Fano coherences generated by polarized incoherent excitation do not vanish in the steady state $(t \to \infty)$ unlike those in isotropic excitation. This is a result of the imbalance between polarized incoherent excitation and spontaneous emission (the former is directional, whereas the latter is isotropic), leading to a breakdown of detailed balance and the emergence of non-equilibrium steady-states.[28,40,48] The steady-state populations and coherences (see the supplementary material)

$$\rho_{g_ig_i}^{(\mathrm{SS})} = \frac{(r+\gamma)\Delta^2 + r^2\gamma}{(3r+2\gamma)\Delta^2 + 2r^2\gamma},$$
$$\rho_{g_1g_2}^{R(\mathrm{SS})} = -\frac{r^2\gamma}{(3r+2\gamma)\Delta^2 + 2r^2\gamma} \tag{9}$$

deviate from the values expected in thermal equilibrium $[\rho_{g_ig_i}^{(\mathrm{SS,th})} = (r+\gamma)/(3r+2\gamma)]$. As in the case of the V-system,[40] this could be used to detect Fano coherences by measuring the deviation of steady-state populations from their expected equilibrium values.

IV. SUMMARY

We have explored the quantum dynamics of noise-induced Fano coherences in a prototypical three-level Λ-system driven by BBR. In contrast to its V-system counterpart,[4,27–29] the weakly driven Λ-system almost always remains in the underdamped regime characterized by oscillatory coherence dynamics that decays on the timescale $1/r$ (for $\Delta/\gamma \gg 1$) or $2/r$ (for $\Delta/\gamma \ll 1$), which can be extremely long for small pumping rates $r/\gamma \simeq 10^{-9}$ relevant for photosynthetic solar light harvesting.[4,52] This also suggests that Fano coherences may find applications in, e.g., quantum sensing,[59] where a qubit's coherence time is a key figure of merit. Similarly, the long-lived coherent quasi-steady states that arise in the strongly driven Λ-system (see Fig. 2) have a lower entropy than the corresponding thermal states, motivating further research into the origin and potential utility of these states [as well as the true coherent steady states shown in Fig. 3(b)] in multilevel quantum systems.

While both the V-system and the Λ-system have a pair of nearly degenerate levels, the crucial difference between them is that the nearly degenerate levels of the V-system are subject to spontaneous emission, whereas those of the Λ-system are not. As a consequence, these systems exhibit very different noise-driven dynamics in the regime, where the spontaneous emission rate is much higher than the incoherent driving rate. This occurs in the weakly driven regime $(r/\gamma \ll 1)$ of importance for photosynthetic light-harvesting under ambient sunlight conditions. On the other hand, if the rate of spontaneous emission is smaller than that of incoherent pumping (the strongly driven regime, $r/\gamma \gg 1$), then one might expect the V-system and Λ-system to display similar dynamical features as is, indeed, the case. One notable example is provided by the long-lived coherent quasi-steady states, which have exactly the same lifetimes for both the V-system and Λ-system, and can be described by the same effective decoherence rate model.[29]

In addition to similar dynamical behavior, the mathematical features of both models in the strongly driven regime are fairly similar. For instance, the zero-discriminant equation of the strongly driven Λ-system given by Eq. (21) of the supplementary material is the same as that of the V-system. Furthermore, the expressions for the population and coherence dynamics of the strongly driven Λ- and V-systems have the same form when expressed in terms of the coefficients A_i, B_i, and C_i (see the supplementary material,

Sec. I.E.2). Nevertheless, these coefficients have a completely different dependence on the transition dipole alignment factor p for the V-system and the Λ-system.

Finally, we propose an experimental scenario for detecting Fano coherences by driving circularly polarized ${}^3S_{m=\pm1} \leftrightarrow {}^3P_0$ transitions in metastable He atoms excited by x-polarized incoherent radiation and subject to an external magnetic field. Our results suggest that thermal driving can lead to novel long-lived quantum beats and non-thermal coherent steady states in multilevel atomic and molecular systems, motivating further studies of Fano coherences in more complex multilevel molecular systems and of their role in photosynthetic energy transfer processes and in quantum information science.

SUPPLEMENTARY MATERIAL

See the supplementary material for a detailed derivation of the analytical solutions of the BR equations presented in the main text.

ACKNOWLEDGMENTS

We thank Professor Amar Vutha for suggesting He* as an experimental realization of the Λ-system and Professor Paul Brumer for a valuable discussion. This work was partially supported by the NSF under Grant No. PHY-1912668.

AUTHOR DECLARATIONS

Conflict of Interest

The authors have no conflicts to disclose.

Author Contributions

Suyesh Koyu: Investigation (lead); Methodology (lead); Validation (lead); Visualization (lead); Writing – original draft (supporting); Writing – review & editing (supporting). **Timur V. Tscherbul**: Conceptualization (lead); Project administration (lead); Supervision (lead); Writing – original draft (lead); Writing – review & editing (lead).

DATA AVAILABILITY

The data that support the findings of this study are available from the corresponding author upon reasonable request.

REFERENCES

[1]P. Brumer, "Shedding (incoherent) light on quantum effects in light-induced biological processes," J. Phys. Chem. Lett. **9**, 2946 (2018).
[2]J. Cao, R. J. Cogdell, D. F. Coker, H. G. Duan, J. Hauer, U. Kleinekathöfer, T. L. C. Jansen, T. Mančal, R. J. D. Miller, J. P. Ogilvie, V. I. Prokhorenko, T. Renger, H. S. Tan, R. Tempelaar, M. Thorwart, E. Thyrhaug, S. Westenhoff, and D. Zigmantas, "Quantum biology revisited," Sci. Adv. **6**, eaaz4888 (2020).
[3]A. Dodin and P. Brumer, "Noise-induced coherence in molecular processes," J. Phys. B: At., Mol. Opt. Phys. **54**, 223001 (2021).
[4]T. V. Tscherbul and P. Brumer, "Long-lived quasistationary coherences in a V-type system driven by incoherent light," Phys. Rev. Lett. **113**, 113601 (2014).
[5]J. Olšina, A. G. Dijkstra, C. Wang, and J. Cao, "Can natural sunlight induce coherent exciton dynamics?," arXiv:1408.5385 (2014).
[6]R. Kosloff and A. Levy, "Quantum heat engines and refrigerators: Continuous devices," Annu. Rev. Phys. Chem. **65**, 365 (2014).
[7]M. O. Scully, K. R. Chapin, K. E. Dorfman, M. B. Kim, and A. Svidzinsky, "Quantum heat engine power can be increased by noise-induced coherence," Proc. Natl. Acad. Sci. U. S. A. **108**, 15097 (2011).
[8]K. E. Dorfman, D. V. Voronine, S. Mukamel, and M. O. Scully, "Photosynthetic reaction center as a quantum heat engine," Proc. Natl. Acad. Sci. U. S. A. **110**, 2746 (2013).
[9]K. Beloy, U. I. Safronova, and A. Derevianko, "High-accuracy calculation of the blackbody radiation shift in the ^{133}Cs primary frequency standard," Phys. Rev. Lett. **97**, 040801 (2006).
[10]M. S. Safronova, M. G. Kozlov, and C. W. Clark, "Blackbody radiation shifts in optical atomic clocks," IEEE Trans. Ultrason., Ferroelectr., Freq. Control **59**, 439 (2012).
[11]V. D. Ovsiannikov, A. Derevianko, and K. Gibble, "Rydberg spectroscopy in an optical lattice: Blackbody thermometry for atomic clocks," Phys. Rev. Lett. **107**, 093003 (2011).
[12]C. Lisdat, S. Dörscher, I. Nosske, and U. Sterr, "Blackbody radiation shift in strontium lattice clocks revisited," Phys. Rev. Res. **3**, L042036 (2021).
[13]I. Kassal, J. Yuen-Zhou, and S. Rahimi-Keshari, "Does coherence enhance transport in photosynthesis?," J. Phys. Chem. Lett. **4**, 362 (2013).
[14]R. d. J. León-Montiel, I. Kassal, and J. P. Torres, "Importance of excitation and trapping conditions in photosynthetic environment-assisted energy transport," J. Phys. Chem. B **118**, 10588 (2014).
[15]T. V. Tscherbul and P. Brumer, "Non-equilibrium stationary coherences in photosynthetic energy transfer under weak-field incoherent illumination," J. Chem. Phys. **148**, 124114 (2018).
[16]P.-Y. Yang and J. Cao, "Steady-state analysis of light-harvesting energy transfer driven by incoherent light: From dimers to networks," J. Phys. Chem. Lett. **11**, 7204 (2020).
[17]C. Chuang and P. Brumer, "LH1–RC light-harvesting photocycle under realistic light–matter conditions," J. Chem. Phys. **152**, 154101 (2020).
[18]D. Polli, P. Altoè, O. Weingart, K. M. Spillane, C. Manzoni, D. Brida, G. Tomasello, G. Orlandi, P. Kukura, R. A. Mathies, M. Garavelli, and G. Cerullo, "Conical intersection dynamics of the primary photoisomerization event in vision," Nature **467**, 440 (2010).
[19]K. Schulten and S. Hayashi, "Quantum biology of retinal," in *Quantum Effects in Biology*, edited by G. S. Engel, M. B. Plenio, M. Mohseni, and Y. Omar (Cambridge University Press, Cambridge, 2014), pp. 237–263.
[20]T. V. Tscherbul and P. Brumer, "Excitation of biomolecules with incoherent light: Quantum yield for the photoisomerization of model retinal," J. Phys. Chem. A **118**, 3100 (2014).
[21]T. V. Tscherbul and P. Brumer, "Quantum coherence effects in natural light-induced processes: *cis–trans* photoisomerization of model retinal under incoherent excitation," Phys. Chem. Chem. Phys. **17**, 30904 (2015).
[22]C. Chuang and P. Brumer, "Steady state photoisomerization quantum yield of model rhodopsin: Insights from wavepacket dynamics?," J. Phys. Chem. Lett. **13**, 4963 (2022).
[23]C. Cohen-Tannoudji, J. Dupont-Roc, and G. Grynberg, *Atom-Photon Interactions: Basic Processes and Applications* (Wiley-VCH, 2004).
[24]K. Blum, *Density Matrix Theory and Applications* (Springer, 2011), Chap. 8.
[25]F. K. Wilhelm, M. J. Storcz, U. Hartmann, and M. R. Geller, "Superconducting qubits II: Decoherence," in *Manipulating Quantum Coherence in Solid State Systems*, edited by M. E. Flatté and I. Ţifrea (Springer Netherlands, Dordrecht, 2007), pp. 195–232.
[26]J. Jeske, D. J. Ing, M. B. Plenio, S. F. Huelga, and J. H. Cole, "Bloch-Redfield equations for modeling light-harvesting complexes," J. Chem. Phys. **142**, 064104 (2015).
[27]A. Dodin, T. V. Tscherbul, and P. Brumer, "Quantum dynamics of incoherently driven V-type systems: Analytic solutions beyond the secular approximation," J. Chem. Phys. **144**, 244108 (2016).

[28]A. Dodin, T. V. Tscherbul, R. Alicki, A. Vutha, and P. Brumer, "Secular versus nonsecular Redfield dynamics and Fano coherences in incoherent excitation: An experimental proposal," Phys. Rev. A **97**, 013421 (2018).
[29]S. Koyu and T. V. Tscherbul, "Long-lived quantum coherences in a V-type system strongly driven by a thermal environment," Phys. Rev. A **98**, 023811 (2018).
[30]T. V. Tscherbul and P. Brumer, "Partial secular Bloch-Redfield master equation for incoherent excitation of multilevel quantum systems," J. Chem. Phys. **142**, 104107 (2015).
[31]P. R. Eastham, P. Kirton, H. M. Cammack, B. W. Lovett, and J. Keeling, "Bath-induced coherence and the secular approximation," Phys. Rev. A **94**, 012110 (2016).
[32]Z. Wang, W. Wu, and J. Wang, "Steady-state entanglement and coherence of two coupled qubits in equilibrium and nonequilibrium environments," Phys. Rev. A **99**, 042320 (2019).
[33]C.-Y. Liao and X.-T. Liang, "The Lindblad and Redfield forms derived from the Born–Markov master equation without secular approximation and their applications," Commun. Theor. Phys. **73**, 095101 (2021).
[34]M. Merkli, H. Song, and G. P. Berman, "Multiscale dynamics of open three-level quantum systems with two quasi-degenerate levels," J. Phys. A: Math. Theor. **48**, 275304 (2015).
[35]A. Trushechkin, "Unified Gorini-Kossakowski-Lindblad-Sudarshan quantum master equation beyond the secular approximation," Phys. Rev. A **103**, 062226 (2021).
[36]M. Fleischhauer, C. H. Keitel, M. O. Scully, and C. Su, "Lasing without inversion and enhancement of the index of refraction via interference of incoherent pump processes," Opt. Commun. **87**, 109 (1992).
[37]G. C. Hegerfeldt and M. B. Plenio, "Coherence with incoherent light: A new type of quantum beat for a single atom," Phys. Rev. A **47**, 2186 (1993).
[38]V. V. Kozlov, Y. Rostovtsev, and M. O. Scully, "Inducing quantum coherence via decays and incoherent pumping with application to population trapping, lasing without inversion, and quenching of spontaneous emission," Phys. Rev. A **74**, 063829 (2006).
[39]B.-Q. Ou, L.-M. Liang, and C.-Z. Li, "Coherence induced by incoherent pumping field and decay process in three-level Λ-type atomic system," Opt. Commun. **281**, 4940 (2008).
[40]S. Koyu, A. Dodin, P. Brumer, and T. V. Tscherbul, "Steady-state Fano coherences in a V-type system driven by polarized incoherent light," Phys. Rev. Res. **3**, 013295 (2021).
[41]Z. Ficek and S. Swain, *Quantum Interference and Coherence: Theory and Experiments* (Springer-Verlag, New York, 2005).
[42]A. K. Patnaik and G. S. Agarwal, "Cavity-induced coherence effects in spontaneous emissions from preselection of polarization," Phys. Rev. A **59**, 3015 (1999).
[43]K. T. Kapale, M. O. Scully, S.-Y. Zhu, and M. S. Zubairy, "Quenching of spontaneous emission through interference of incoherent pump processes," Phys. Rev. A **67**, 023804 (2003).
[44]K. A. Jung and P. Brumer, "Energy transfer under natural incoherent light: Effects of asymmetry on efficiency," J. Chem. Phys. **153**, 114102 (2020).
[45]V. Janković and T. Mančal, "Nonequilibrium steady-state picture of incoherent light-induced excitation harvesting," J. Chem. Phys. **153**, 244110 (2020).
[46]S. Tomasi, D. M. Rouse, E. M. Gauger, B. W. Lovett, and I. Kassal, "Environmentally improved coherent light harvesting," J. Phys. Chem. Lett. **12**, 6143 (2021).
[47]C. L. Latune, I. Sinayskiy, and F. Petruccione, "Negative contributions to entropy production induced by quantum coherences," Phys. Rev. A **102**, 042220 (2020).
[48]G. S. Agarwal and S. Menon, "Quantum interferences and the question of thermodynamic equilibrium," Phys. Rev. A **63**, 023818 (2001).
[49]H. S. Han, A. Lee, K. Sinha, F. K. Fatemi, and S. L. Rolston, "Observation of vacuum-induced collective quantum beats," Phys. Rev. Lett. **127**, 073604 (2021).
[50]M. Fleischhauer, A. Imamoglu, and J. P. Marangos, "Electromagnetically induced transparency: Optics in coherent media," Rev. Mod. Phys. **77**, 633 (2005).
[51]T. P. Altenmüller, "Are there quantum beats from vacuum-induced coherence?," Z. Phys. D: At., Mol. Clusters **34**, 157 (1995).
[52]K. Hoki and P. Brumer, "Excitation of biomolecules by coherent vs. incoherent light: Model rhodopsin photoisomerization," Procedia Chem. **3**, 122 (2011).
[53]H.-P. Breuer and F. Petruccione, *The Theory of Open Quantum Systems* (Clarendon Press, Oxford, 2006).
[54]G. McCauley, B. Cruikshank, D. I. Bondar, and K. Jacobs, "Accurate Lindblad-form master equation for weakly damped quantum systems across all regimes," npj Quantum Inf. **6**, 74 (2020).
[55]A. Dodin, T. V. Tscherbul, and P. Brumer, "Coherent dynamics of V-type systems driven by time-dependent incoherent radiation," J. Chem. Phys. **145**, 244313 (2016).
[56]A. Dodin and P. Brumer, "Generalized adiabatic theorems: Quantum systems driven by modulated time-varying fields," PRX Quantum **2**, 030302 (2021).
[57]W. Vassen, C. Cohen-Tannoudji, M. Leduc, D. Boiron, C. I. Westbrook, A. Truscott, K. Baldwin, G. Birkl, P. Cancio, and M. Trippenbach, "Cold and trapped metastable noble gases," Rev. Mod. Phys. **84**, 175 (2012).
[58]W. Vassen, R. P. M. J. W. Notermans, R. J. Rengelink, and R. F. H. J. van der Beek, "Ultracold metastable helium: Ramsey fringes and atom interferometry," Appl. Phys. B **122**, 289 (2016).
[59]C. L. Degen, F. Reinhard, and P. Cappellaro, "Quantum sensing," Rev. Mod. Phys. **89**, 035002 (2017).